Journal of Medicinal Chemistry

Article

pubs.acs.org/jmc

Novel Cyclopentadienyl Tricarbonyl Complexes of ^{99m}Tc Mimicking Chalcone as Potential Single-Photon Emission Computed Tomography Imaging Probes for β-Amyloid Plaques in Brain

Zijing Li,[†] Mengchao Cui,*[,†] Jiapei Dai,[‡] Xuedan Wang,[†] Pingrong Yu,[†] Yanping Yang,[†] Jianhua Jia,[†] Hualong Fu,[†] Masahiro Ono,[§] Hongmei Jia,[†] Hideo Saji,[§] and Boli Liu*[,†]

[†]Key Laboratory of Radiopharmaceuticals, Ministry of Education, College of Chemistry, Beijing Normal University, Beijing 100875, P. R. China

[‡]Wuhan Institute for Neuroscience and Neuroengineering, South-Central University for Nationalities, Wuhan 430074, P. R. China

[§]Department of Patho-Functional Bioanalysis, Graduate School of Pharmaceutical Sciences, Kyoto University, 46-29 Yoshida Shimoadachi-cho, Sakyo-ku, Kyoto 606-8501, Japan

Supporting Information

ABSTRACT: Rhenium and technetium-99m cyclopentadienyl tricarbonyl complexes mimicking the chalcone structure were prepared. These complexes were proved to have affinity to β-amyloid (Aβ) in fluorescent staining on brain sections of Alzheimer's Disease (AD) patient and binding assay using $A\beta_{1-42}$ aggregates, with K_i values ranging from 899 to 108 nM as the extension of conjugated π system. In vitro autoradiograpy on sections of transgenic mouse brain confirmed the affinity of [^{99m}Tc]**5** (K_i = 108 nM). In biodistribution, all compounds showed good initial uptakes into the brain and fast blood clearance, while the decreasing of initial brain uptakes correspond to increasing of conjugation length, from 4.10 ± 0.38% ID/g ([^{99m}Tc]**3**) to 1.11 ± 0.34% ID/g ([^{99m}Tc]**5**). These small technetium-99m complexes (<500 Da) designed by an integrated approach provide encouraging evidence that development of a promising ^{99m}Tc-labeled agent for imaging Aβ plaques in the brain may be feasible.

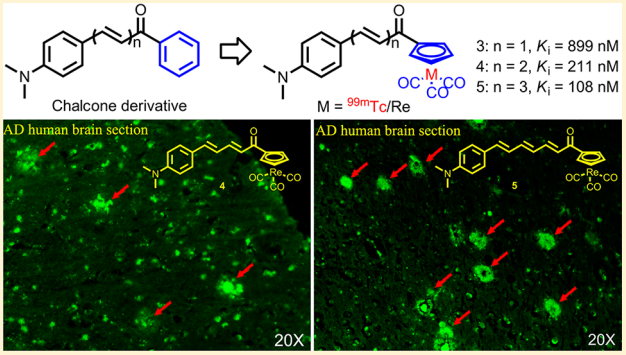

INTRODUCTION

Alzheimer's disease (AD) is a progressive neurodegenerative disorder pathologically characterized by deposition of misfolded β-amyloid (Aβ) peptides as senile plaques in the brain. Because the deposition of Aβ plaques is an early event in the development of AD, a validated biomarker of Aβ deposition in the brain might prove useful to identify and follow individuals at risk for AD and to assist in the evaluation of new antiamyloid therapies currently under development.[1−3]

A number of groups have reported radiolabeled Aβ imaging agents for positron emission tomography (PET) and single photon emission computed tomography (SPECT) in clinical trials such as [^{18}F]FDDNP ([^{18}F]-2-(1-(6-[(2-fluoroethyl)-(methyl)amino]-2-naphthyl)ethylidene)malononitrile),[4,5] [^{11}C]PIB ([^{11}C]-2-(4′-methylaminophenyl)-6-oxybenzothiazole),[6,7] [^{11}C]SB-13 ([^{11}C]-4-*N*-methylamino-4′-hydroxystilbene),[8,9] [^{11}C]BF-227 ([^{11}C]-(2-[fluoro]ethoxy)-benzoxazole),[10] [^{18}F]BAY94−9172 ([^{18}F]-4-(*N*-methylamino)-4′-(2-(2-(2-fluoroethoxy)ethoxy)ethoxy)-stilbene),[11] [^{18}F]AV-45 ([^{18}F]-(*E*)-4-(2-(6-(2-(2-(2-fluoroethoxy)ethoxy)-ethoxy)pyridin-3-yl)vinyl)-*N*-methylaniline),[12,13] and [^{123}I]IMPY ([^{123}I]-6-iodo-2-(4′-dimethylamino-)phenyl-imidazo[1,2]pyridine).[14−16] Recent reports using these amyloid imaging agents have indicated that detecting Aβ plaques in the living human brain by PET or SPECT may lead to differentiation between AD patients and healthy humans. However, the signal-to-noise ratio for plaque labeling of [^{123}I]IMPY, which is the only SPECT Aβ imaging agents in preclinical trail, was not robust in AD and healthy controls, while it was believed that the in vivo instability and fast metabolism of [^{123}I]IMPY may ultimately lead to a decreased signal. After that, there is no report of any Aβ imaging candidate for SPECT moving into clinical trial.

However, the radionuclide technetium-99m is among the most widely used isotopes in diagnostic nuclear medicine. Readily produced by a ^{99}Mo/^{99m}Tc generator, essentially 24 h/day, ^{99m}Tc emits medium γ-ray energy suitable for detection, and its physical half-life is compatible with the biological localization and residence time required for imaging. New ^{99m}Tc-labeled imaging agents for Aβ plaques will provide simple, convenient and widespread SPECT-based imaging methods for detecting and eventually quantifying Aβ plaques in living brain tissue,[17−19] whereas in the past ^{99m}Tc complexes

Received: September 29, 2012
Published: December 14, 2012

   dx.doi.org/10.1021/jm3014184 | J. Med. Chem. 2013, 56, 471−482

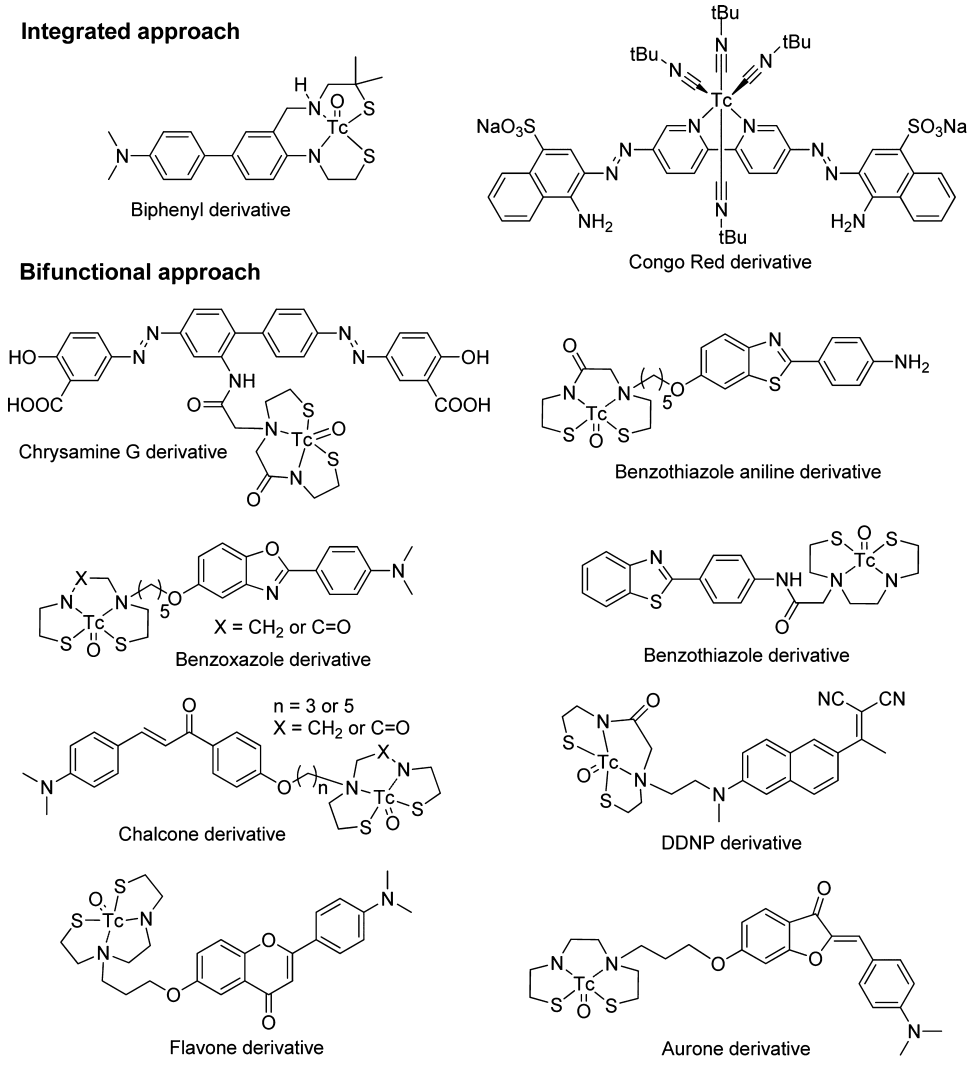

Figure 1. Chemical structures of reported ^{99m}Tc labeled Aβ imaging probes.

were preferentially applied as perfusion agents. A challenge now lies in combining a ^{99m}Tc complex with a targeting molecule such as a small central nervous system (CNS) receptor-binding molecule.

Kung et al. reported that the dopamine transporter imaging agent [^{99m}Tc]TRODAT-1[20] is useful to detect the loss of dopamine transporters in Parkinson's disease. This is the first example of a ^{99m}Tc imaging agent that can penetrate the blood−brain barrier (BBB) via a simple diffusion mechanism and localize at receptor binding sites in the CNS. On the basis of this success, efforts were made to search for comparable ^{99m}Tc imaging agents that target binding sites on Aβ plaques in the brain of AD patients. Several ^{99m}Tc-labeled imaging probes have been developed (Figure 1). Two of them are based on an integrated approach (the Congo Red derivative[21] and the biphenyl derivative[22]). The integrated approach involves the replacement of part of a known high-affinity receptor ligand with the requisite "unnatural" ^{99m}Tc chelate in such a way that there are minimal changes in size, conformation, and receptor binding affinity.[23] The others are based on a bifunctional approach (the chrysamine G derivative,[24,25] the benzothiazole aniline derivative,[26−28] the chalcone derivative,[29] the flavone and aurone derivative,[30] the benzoxazole derivative,[31] the DDNP derivative,[32] etc.). The bifunctional approach leads to volume expansion. This expansion twists the planar shape of the binding agent, which is very important for a molecular agent to fit into the planar gap on the Aβ plaques and also increases the molecular weight greatly. Conversely, the integrated approach strategy seems wiser but more difficult to practice. Unfortunately, no clinical study of both kinds has been reported because the low initial brain uptake is not sufficient for SPECT imaging, even if they display high affinities to Aβ.

On the basis of the discovery so far, the best strategy to design Aβ imaging agents is to find an small, lipophilic, ^{99m}Tc-chelating core to substitute or mimic one part of the structure of a binding agent by integrated approach in order to maintain the planar shape of the ligand, minimize the molecular weight, and maintain the ability to penetrate the BBB.

As early as 1992, Wenzel reported a double ligand transfer (DLT) reaction,[33] which ultimately led to the formation of [Cp^{99m}Tc(CO)$_3$, Cp = cyclopentadienyl] starting from ^{99m}TcO$_4^-$. Then the method of preparing [Cp^{99m}Tc(CO)$_3$] in water has been developed using sensitive organometallic ligands.[34] Apart from this feasibility consideration, the cyclopentadienyl tricarbonyl ligand offers very attractive properties as a ligand for radiopharmaceutical purposes. Its inherent advantages are the small size, the low molecular weight, and the high stability of half-sandwich configuration and the minimized

dx.doi.org/10.1021/jm3014184 | J. Med. Chem. 2013, 56, 471−482

steric interference with the receptor binding moiety of a labeled biomolecule.[35] The "piano stool" organometallic core [CpM(CO)$_3$, M = Re(I), Tc(I)] is a neutral 18 electron species, with high stability resulting from the low-spin d^6 electron configuration, further stabilized by the cyclopentadienyl and tricarbonyl ligands. Although many highly stable chelate systems have been developed for ^{99m}Tc, the small size of the [CpM(CO)$_3$] core is advantageous for maintaining biological activity, particularly when labeling small molecules. The fact that [CpM(CO)$_3$] (M = Re and Tc) can be coupled to biomolecules by classical organometallic methods without affecting the bioactivity has been demonstrated by several groups.[34] Furthermore, [Cp^{99m}Tc(CO)$_3$] complexes are highly lipophilic, which makes them particularly promising as ^{99m}Tc-labeled, BBB-crossing molecules. So, taking the configuration and aromatic properties of [Cp^{99m}Tc(CO)$_3$] core into consideration, it is an excellent choice to substitute or mimic a benzene ring of a ligand by an integrated approach.

Ono et.al. reported in 2007 that chalcone derivatives,[36] whose backbone structure is considered to be a promising scaffold, showed excellent characteristics as new amyloid imaging agents, such as high binding affinity to Aβ aggregates, high uptake into the brain, and rapid clearance from the brain, besides it can easily be formed by one-pot condensation reaction.

After ^{125}I-, ^{11}C-, and ^{18}F-labeled chalcone derivatives were prepared and chalcone scaffold were proved promising candidate as AD imaging agent,[36−38] additionally, in 2010, the same group reported synthesis of four chalcone derivatives with monoamine−monoamide dithiol (MAMA) and bis-amino-bis-thiol (BAT) selected as chelation ligands by bifunctional approach. For the first time, ^{99m}Tc/Re complexes as chalcone derivatives have been proposed as probes for the detection of Aβ plaques in the brain.[29] In their study, MAMA and BAT were selected as chelation ligands to form an electrically neutral complex with ^{99m}Tc, but these two big chelating groups increase the molecular weight and also decrease the affinities and initial brain uptakes as well.

In the present study, we designed and synthesized novel chalcone-mimic complexes by introducing [Cp^{99m}Tc(CO)$_3$] core to substitute a benzene ring (Figure 2) by an integrated approach in order to acquire good brain uptake while keeping excellent affinities to Aβ plaques. Furthermore, the properties of this series of ^{99m}Tc/Re complexes were studied as the extension of conjugated π system.

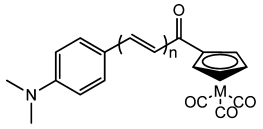

M = ^{99m}Tc/Re, n = 1, 2, 3

Figure 2. Chemical structure of the designed ^{99m}Tc/Re labeled [RCOCpM(CO)$_3$] (M = ^{99m}Tc/Re) complexes.

RESULTS AND DISCUSSION

Chemistry. For characterization of the ^{99m}Tc complexes, we have prepared the corresponding rhenium complexes (Scheme 1). To collect the three corresponding aromatic aldehydes, the aromatic aldehyde **1** was prepared by Wittig reaction from (*E*)-3-(4-(dimethylamino)phenyl)acrylaldehyde, which is commercially available. (Cyclopentadienyl)tricarbonylrhenium was at first acetylated by acetyl chloride in ice bath to obtain (acetylcyclopentadienyl)tricarbonylrhenium (**2**) at 95% yield. This complex can react with three aromatic aldehydes respectively through base-catalyzed Claisen condensation to obtain final rhenium complexes (**3**, **4**, and **5**) of different π conjugation length at yields above 90%. By the way, two ferrocene complexes (**6** and **7**) were synthesized through the same method as precursors for [^{99m}Tc]**4** and [^{99m}Tc]**5**. All these complexes were fully characterized by spectroscopic methods. Complexes **3** and **4** could be recrystallized by slow evaporation of an ethanol−CH_2Cl_2 solution to afford X-ray quality crystals. The structures were elucidated and their ORTEPs are given in Figures 3 and 4, with relevant crystallographic data in Table 1.

Scheme 1[a]

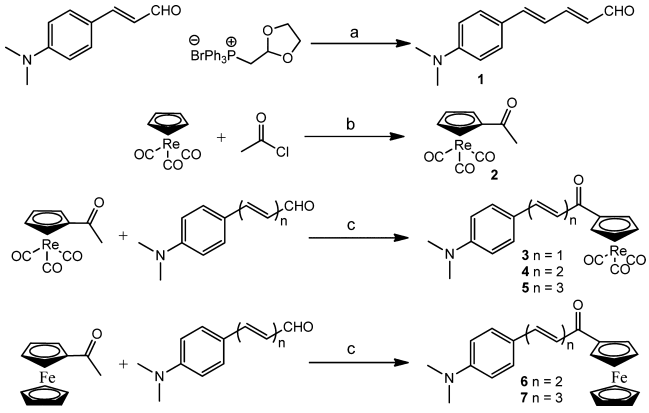

[a]Reagents and conditions: (a) (1) NaH, 18-crown-6, dry THF, r.t., (2) concentrated HCl, K_2CO_3 aq r.t.; (b) $COCl_2$, $AlCl_3$, CH_2Cl_2; (c) NaOH, EtOH, r.t.

Radiolabeling. To get the ^{99m}Tc-labeled cyclopentadienyl tricarbonyl complexes [^{99m}Tc]**3**, [^{99m}Tc]**4**, and [^{99m}Tc]**5**, a two-step sequential reaction (Scheme 2) has to be applied. In the first step, we prepared [$CH_3COCp^{99m}Tc(CO)_3$] ([^{99m}Tc]**2**) under 150 °C heat for 20 min through the DLT method with an average radiochemical yield of 50% (no decay corrected). Then [^{99m}Tc]**2** went through a base-catalyzed Claisen condensation with three corresponding aldehydes to yield [^{99m}Tc]**3**, [^{99m}Tc]**4**, and [^{99m}Tc]**5**. The final ^{99m}Tc-labeled products were purified by radio high performance liquid chromatography (HPLC), and the identity of [^{99m}Tc]**3**, [^{99m}Tc]**4**, and [^{99m}Tc]**5** was verified by a comparison of the retention time with that of the nonradioactive rhenium compounds (Figures 5, 6, and 7). In the second step, the radiochemical yields of [^{99m}Tc]**3**−**5** were also about 50% (no decay corrected), to achieve a 25% total yield with radiochemical purity of >95% after HPLC purification. We took this two-step strategy because the direct DLT labeling method under 150 °C would destroy the ferrocene precursor (**6** and **7**) and give no products. Furthermore, this radiochemical synthesis by Claisen condensation strategy was proved brilliant in the following experiments because the reaction was not only fast enough for ^{99m}Tc labeling but also ready to be applied to label many different aldehyde or large molecules which contain aldehyde groups with [Cp^{99m}Tc(CO)$_3$] core at acceptable yields.

Biological Evaluation. In vitro fluorescent staining of Aβ plaques in sections of brain tissue from AD patients and Tg model mice (C57BL6, APPswe/PSEN1, 11 months old) were

dx.doi.org/10.1021/jm3014184 | J. Med. Chem. 2013, 56, 471−482

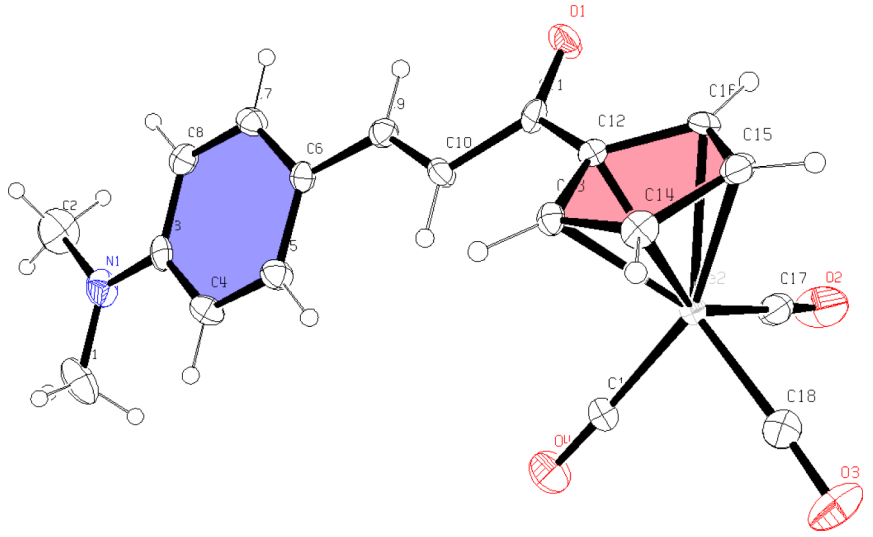

Figure 3. Molecular structure of **3** (thermal ellipsoids drawn at the 30% probability level).

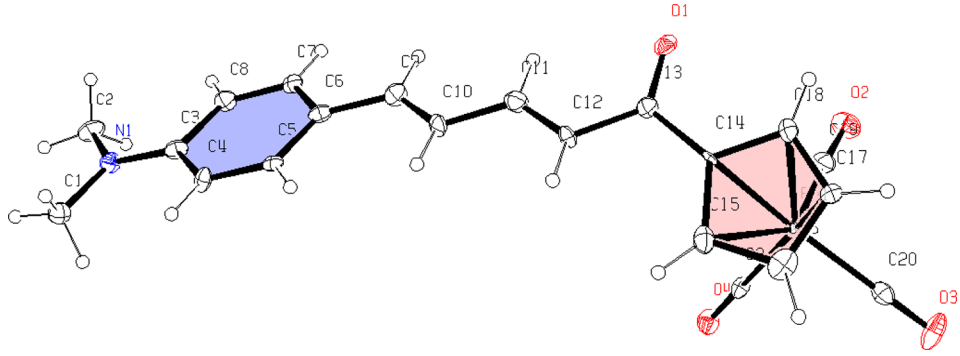

Figure 4. Molecular structure of **4** (thermal ellipsoids drawn at the 30% probability level).

Table 1. Summary of X-ray Crystallographic Data

	3	4
formula sum	$C_{19}H_{16}NO_4Re$	$C_{21}H_{18}NO_4Re$
formula weight (g/mol)	508.53	534.56
crystal system	triclinic	orthorhombic
space group	$P\bar{1}$ (2)	*Pca*21 (29)
a (Å)	5.9756(8)	12.730(2)
b (Å)	11.8247(16)	6.3516(10)
c (Å)	13.6116(19)	12.730(2)
α (deg)	66.46	
β (deg)	78.62	
γ (deg)	80.76	
cell volume (Å^3)	860.82(82)	1845.45(52)
Z	2	4
calcd density (g/cm^3)	1.96182	1.92387
RAll	0.0379	0.0669
Pearson code	aP82	oP180
formula type	NOP4Q16R19	NOP4Q18R21
Wyckoff sequence	i41	a45

carried out to evaluate the binding affinity of complexes **3**, **4**, and **5** to A*β* plaques. As shown in Figure 8A,D, specific staining of plaques were observed in the brain section of Tg mice for complex **4**. The presence and distribution of A*β* plaques was consistent with the results of staining using thioflavin-S (a common dye for staining of A*β* plaques) on the adajacent section (Figure 8B,E). Furthermore, intense labeling of plaques were observed in the brain section of an AD patient (Figure 8G). In contrast, no apparent labeling was observed in both normal mouse and normal adult brain sections (Figure 8C,H) stained by complex **4** (Figure 8F). The similar results of in vitro fluorescent staining of A*β* plaques by complex **5** were showed in Figure 9, while the fluorescent signal stained by complex **3** was weak (data not shown), which may be due to the low affinity.

To quantitatively evaluate the binding affinities of these chalcone-mimic complexes to $A\beta_{1-42}$ aggregates, in vitro inhibition assay was carried out in solutions with [^{125}I]IMPY as the competing radioligand according to conventional methods. The three rhenium complexes (**3**, **4**, and **5**) inhibited the binding of [^{125}I]IMPY in a dose-dependent manner (Figure 10). With the result shown in Table 2, rhenium complexes of different conjugation lengths showed moderate binding affinities to $A\beta_{1-42}$ aggregates (K_i = 899 ± 78 nM for **3**, K_i = 211 ± 19 nM for **4**, and K_i = 108 ± 16 nM for **5**), which are not satisfactory but sufficiently high for A*β* aggregates comparable to the value determined under the same assay system for IMPY (K_i = 10.5 ± 1.0 nM) and chalcone derivatives (with K_i ranged from 2.9 to >10,000 nM as reported[36]). The crystal structures elucidated in Figure 3 and Figure 4 implied that complex **4** is less distorted than complex **3** because the dihedral angle between the benzene plane (light-blue) and the Cp plane (light-red) is 43.69° for complex **3**, while the same dihedral angle of complex **4** is 31.34°. So, we would like to blame the

dx.doi.org/10.1021/jm3014184 | *J. Med. Chem.* 2013, 56, 471−482

Scheme 2[a]

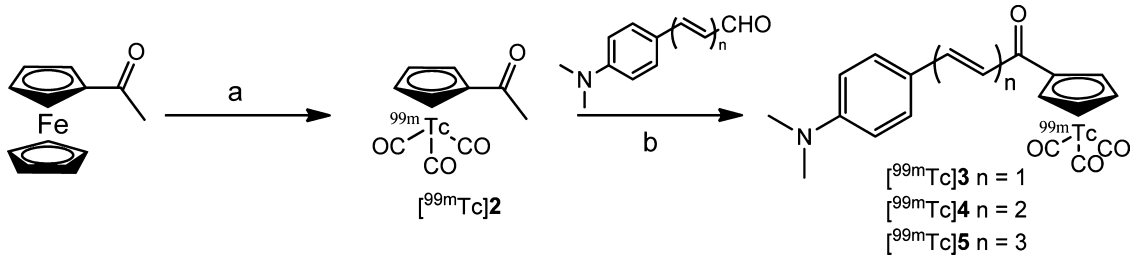

[a]Reagents and conditions: (a) $Mn(CO)_5Br$, $^{99m}TcO_4^-$, H_2O, DMF, 150 °C, 20 min; (b) NaOH, EtOH, r.t.

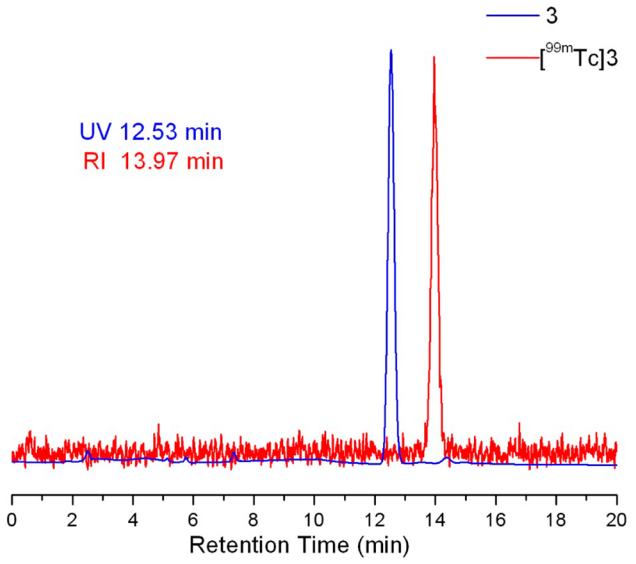

Figure 5. HPLC profiles of **3** and [^{99m}Tc]**3**. HPLC conditions: Venusil MP C18 column (Agela Technologies, 10 mm × 250 mm), CH_3CN/H_2O = 70/30, 4 mL/min, UV, 254 nm.

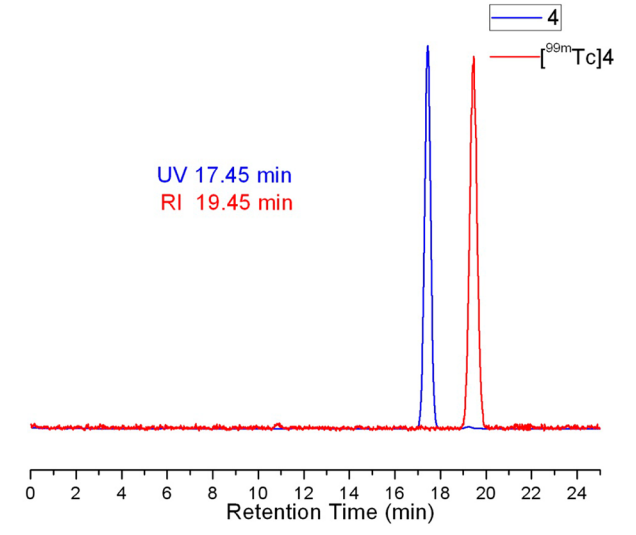

Figure 6. HPLC profiles of **4** and [^{99m}Tc]**4**. HPLC conditions: Venusil MP C18 column (Agela Technologies, 10 mm × 250 mm), CH_3CN/H_2O = 70/30, 4 mL/min, UV, 254 nm.

decreasing of affinity for the three "CO" stools of the [$Cp^{99m}Tc(CO)_3$] core which distort the planar and flake-like configuration of chalcone. Because the K_i values are decreasing as the extension of conjugated π system, we can infer that the extension weakens the influence of the three "CO" stools of the [$Cp^{99m}Tc(CO)_3$] core on the planar configuration. The affinity of the two ferrocene complexes whose structures have no stools still keep high affinity (K_i = 3.36 ± 0.30 nM for **6**, K_i = 5.08 ± 1.74 nM for **7**) also confirm our inference.

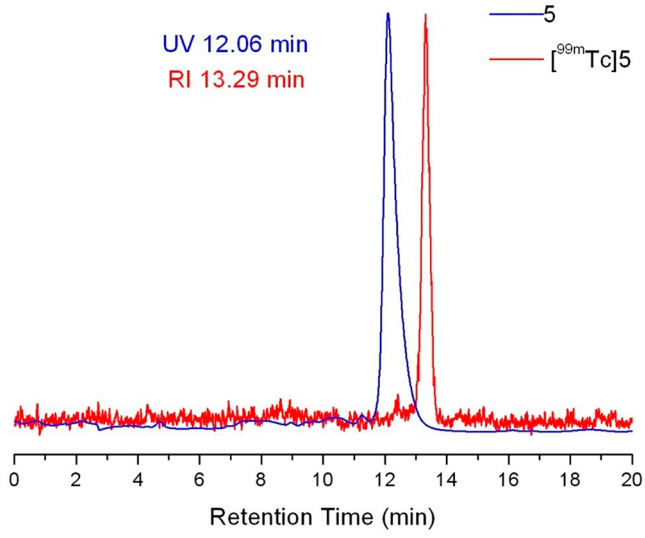

Figure 7. HPLC profiles of **5** and [^{99m}Tc]**5**. HPLC conditions: Venusil MP C18 column (Agela Technologies, 10 mm × 250 mm), CH_3CN/H_2O = 80/20, 4 mL/min, UV, 254 nm.

In binding assays using the aggregated $A\beta_{1-42}$ peptides in solution, we also confirmed that the $A\beta_{1-42}$ aggregate-bound radioactivities (%) were varied differently in the four ^{99m}Tc-labeled complexes. In terms of $A\beta_{1-42}$ aggregate-bound radioactivity, the derivatives rank in the following order: [^{99m}Tc]**5** (10.15%) > [^{99m}Tc]**4** (3.87%) > [^{99m}Tc]**3** (0.68%) > [^{99m}Tc]**2** (0.32%) (Figure 11). Furthermore, the bound radioactivities indicate that [^{99m}Tc]**5** and [^{99m}Tc]**4** occupied the specific binding sites of $A\beta_{1-42}$ aggregates, while [^{99m}Tc]**3** and [^{99m}Tc]**2** showed no remarkable binding to $A\beta_{1-42}$ aggregates. This result suggests that the length of conjugated π system played an important role in the binding of $A\beta_{1-42}$ aggregates, which are also consistent with the binding affinities of these chalcone-mimic complexes in the inhibition assay. The results of blocking assay using excess of rhenium complexes **2**–**5** showed that the specific binding of [^{99m}Tc]**5** to $A\beta_{1-42}$ aggregates was blocked about 80% by an excess of **5** (0.5 μM); the binding of [^{99m}Tc]**4** was blocked nearly a half by an excess of **4** at 1.0 μM, while excess of complexes **3** and **2** at 1.0 μM could not significantly block the binding radioactivity owing to their lower affinities. These results confirmed that complex **5** displayed specific and high binding to $A\beta_{1-42}$ aggregates.

dx.doi.org/10.1021/jm3014184 | J. Med. Chem. 2013, 56, 471–482

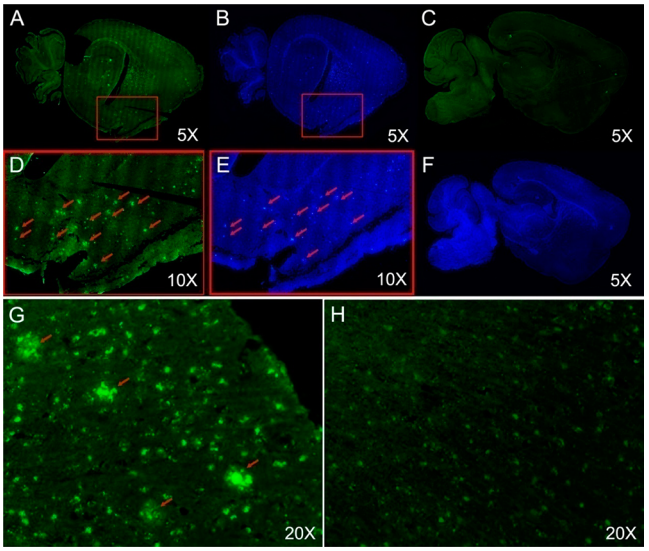

Figure 8. In vitro fluorescent staining of Aβ plaques by complex **4**. (A,D) complex **4** on brain section of a Tg model mouse (C57BL6, APPswe/PSEN1, 11 months old, male); (B,E) the presence and distribution of plaques on the sections were confirmed by fluorescence staining using thioflavin-S on the adjacent section; (C) complex **4** on brain section of a normal mouse as control; (F) thioflavin-S on the adjacent brain section of the normal mouse; (G) complex **4** on brain section of an AD patient (91 years old, male); (H) complex **4** on brain section of a normal person (69 years old, female) as control.

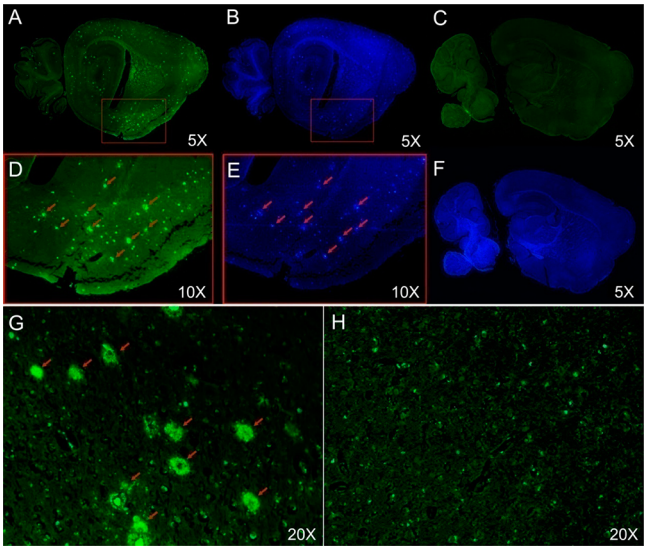

Figure 9. In vitro fluorescent staining of Aβ plaques by complex **5**. (A,D) complex **5** on brain section of a Tg model mouse (C57BL6, APPswe/PSEN1, 11 months old, male); (B,E) the presence and distribution of plaques on the sections were confirmed by fluorescence staining using thioflavin-S on the adjacent section; (C) complex **5** on brain section of a normal mouse as control; (F) thioflavin-S on the adjacent brain section of the normal mouse; (G) complex **5** on brain section of an AD patient (91 years old, male); (H) complex **5** on brain section of a normal person (69 years old, female) as control.

In vitro autoradiography studies of [^{99m}Tc]**5** were performed with sections from Tg mice (C57BL6, APPswe/PSEN1, 11 months old) and an age-matched control mice. As shown in Figure 12, [^{99m}Tc]**5** displayed good labeling of Aβ plaques in the cortical regions of Tg mice, and the control case was clearly void of any notable Aβ labeling. The distribution of Aβ plaques

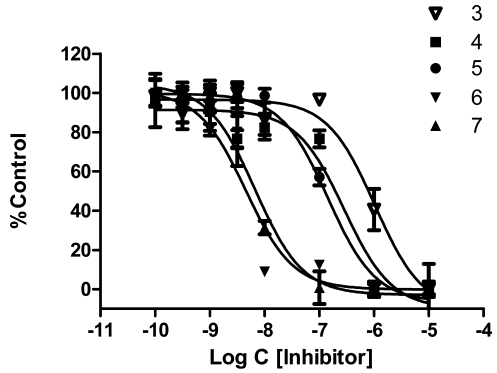

Figure 10. Inhibition curves for the binding of [^{125}I]IMPY to Aβ_{1-42} aggregates.

Table 2. Inhibition Constants (K_i, nM) for Binding to Aggregates of Aβ_{1-42} versus [^{125}I]IMPY[a]

compd	K_i (nM)	compd	K_i (nM)
3	899 ± 78	**6**	3.36 ± 0.30
4	211 ± 19	**7**	5.08 ± 1.74
5	108 ± 16	IMPY	11.5 ± 2.5

[a]Measured in triplicate with results given as the mean ± SD.

was consistent with the results of fluorescent staining with thioflavin-S. Although the binding affinity of [^{99m}Tc]**5** to Aβ aggregates was not potent (K_i = 108 ± 16 nM), [^{99m}Tc]**5** was still able to label the plaques in sections of Tg mice.

The log *D* values (2.89 ± 0.09 for [^{99m}Tc]**3**, 3.61 ± 0.04 for [^{99m}Tc]**4**, and 3.45 ± 0.09 for [^{99m}Tc]**5**, respectively) shown in Table 3 indicate that complexes [^{99m}Tc]**3**, [^{99m}Tc]**4**, and [^{99m}Tc]**5** have moderate lipophilicity suitable for brain imaging.

Biodistribution experiments in normal male ICR mice (5 weeks, male) were carried out to evaluate the ability of these ^{99m}Tc cyclopentadienyl tricarbonyl complexes of different conjugation lengths ([^{99m}Tc]**3**, [^{99m}Tc]**4**, and [^{18}F]**5**) to penetrate the BBB and properties of clearance from the brain. High initial brain uptake and high brain$_{2\ min}$/brain$_{60\ min}$ ratio in normal mouse brain are considered to be important as pharmacokinetic indexes for selecting appropriate Aβ imaging tracers. As shown in Tables 4, 5, and 6, [^{99m}Tc]**3** with a short conjugated π system displayed a very high initial brain uptake (n = 1, 4.10 ± 0.38% ID/g at 2 min) than that of [^{99m}Tc]**4** and [^{99m}Tc]**5** with a longer conjugated π system (n = 2, 2.30 ± 0.27% ID/g at 2 min for [^{99m}Tc]**4**; n = 3, 1.11 ± 0.34% ID/g at 2 min for [^{99m}Tc]**5**). What impressed us was that [^{99m}Tc]**3** exhibits such high initial brain uptake barely not seen before for a ^{99m}Tc-labeled receptor binding agent and that the decreasing of brain uptake is as sharp as the π system extension, where we could not give a good explanation by now. Compared with the ^{99m}Tc-labeled chalcone derivatives (0.22, 0.78, 0.62, 1.48% ID/g at 2 min) by bifunctional approach reported previously,[29] the initial brain uptakes of [^{99m}Tc]**3** and [^{99m}Tc]**4** are apparently superior. Meanwhile, the brain$_{2\ min}$/brain$_{60\ min}$ ratio of 8.20, 4.18, and 2.18 for [^{99m}Tc]**3**, [^{99m}Tc]**4**, and [^{99m}Tc]**5** were from good to acceptable. Furthermore, we can also conclude that [^{99m}Tc]**3**, [^{99m}Tc]**4**, and [^{99m}Tc]**5** are metabolized by liver and small intestine, because the liver showed high uptakes with very slow washout and the small intestine uptakes kept increasing with time.

The biodistribution with permeability-glycoprotein 1 (PgP) blocked by cyclosporin A (an immunosuppressant drug known

dx.doi.org/10.1021/jm3014184 | J. Med. Chem. 2013, 56, 471−482

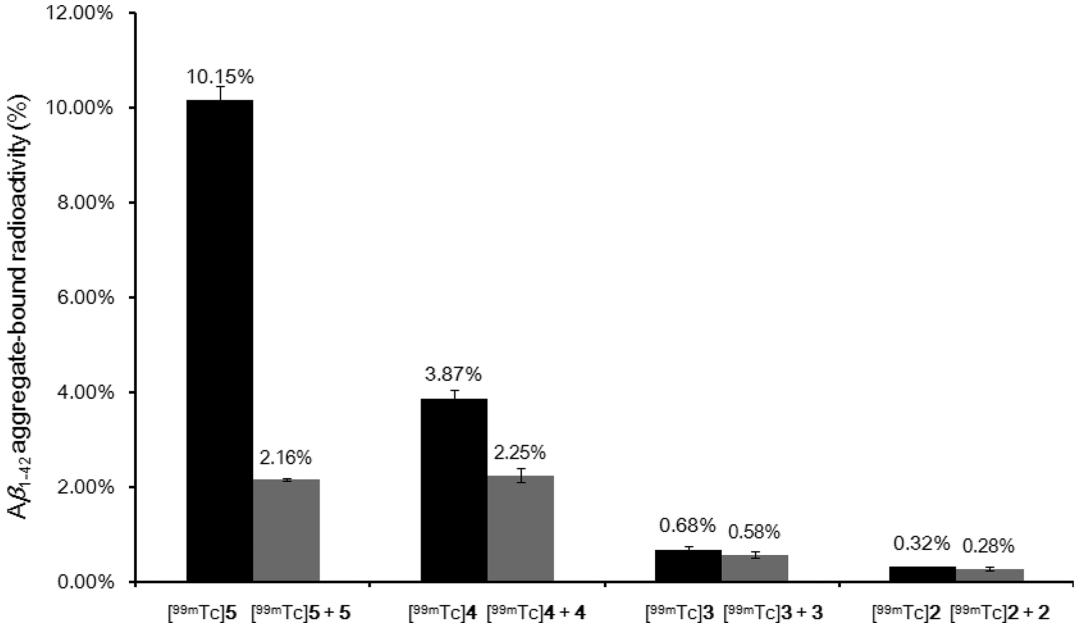

Figure 11. Binding and blocking assay of [^{99m}Tc]**2**, [^{99m}Tc]**3**, [^{99m}Tc]**4**, and [^{99m}Tc]**5** with Aβ_{1-42} aggregates. Values are the mean ± standard error of the mean for tent experiments. Black columns represent the Aβ_{1-42} aggregate-bound radioactivities (%) of [^{99m}Tc]**2**–**5**. Gray columns represent the Aβ_{1-42} aggregate-bound radioactivities (%) of [^{99m}Tc]**2**–**5** blocked by complexes **2**–**4** (1.0 μM) and **5** (0.5 μM), respectively.

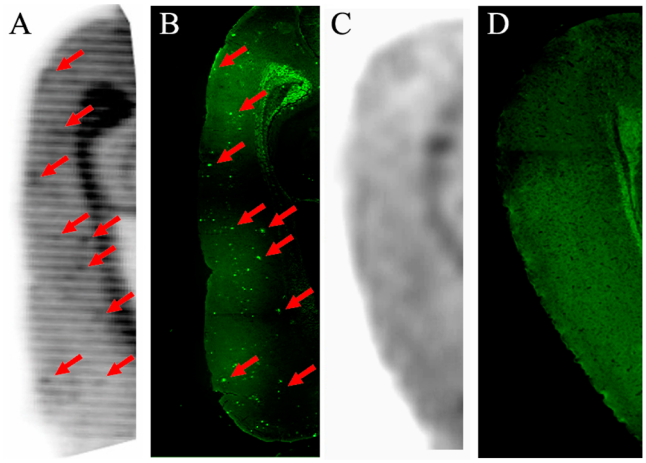

Figure 12. (A) In vitro autoradiography of [^{99m}Tc]**5** on a Tg model mouse (C57BL6, APPswe/PSEN1, 11 months old, male). (B) The presence and distribution of plaques in the section A were confirmed by fluorescence staining using thioflavin-S on the same section with a filter set for GFP. (C) In vitro autoradiography of [^{99m}Tc]**5** on a brain section of a normal mouse (C57BL6, 11 months old, male) as control. (D) Fluorescence staining using thioflavin-S on the section C with a filter set for GFP on a brain section of a normal mouse as control.

Table 3. log *D* Value of Compound [^{99m}Tc]3–5[a]

compd	log *D*
[^{99m}Tc]**3**	2.89 ± 0.09
[^{99m}Tc]**4**	3.61 ± 0.04
[^{99m}Tc]**5**	3.45 ± 0.09

[a]Measured in triplicate with results given as the mean ± SD.

to block PgP activity) further describes their brain penetration abilities. The blood and brain uptakes at 2 min were measured, and the results were shown in Table 7. After the PgP were blocked by cyclosporin A, the brain uptakes of [^{99m}Tc]**3**–**5** increased obviously. This result may reveal [^{99m}Tc]**3**–**5** to be substrates for the rodent PgP transporter.

CONCLUSIONS

Synthesis of organometallic complexes mimicking chalcone structure with ^{99m}Tc cyclopentadienyl tricarbonyl core using a two-step sequential reaction is described in this article. The first step is to prepare the intermediate ([$CH_3COCp^{99m}Tc(CO)_3$]) through the DLT method, and the second step is base-catalyzed Claisen condensation with appropriate aldehydes. We want to emphasize that this pathway can probably be applied to label other aldehydes with a [$Cp^{99m}Tc(CO)_3$] core, especially biomacromolecules, by avoiding the damage of 150 °C heat to the aldehyde in one-step pathway. In vitro fluorescent staining pictures of Aβ plaques on brain sections of patients diagnosed with AD and Tg mouse were clear for complexes **4** and **5**. The binding assay using Aβ_{1-42} aggregates indicated that the K_i value ranges from 899 to 108 nM as the extension of conjugated π system, among which complex **5** has the highest affinity. In vitro autoradiography on section of transgenic mouse brain also confirmed the affinity of [^{99m}Tc]**5** (K_i = 108 nM). In biodistribution, [^{99m}Tc]**3** (4.10 ± 0.38% ID/g at 2 min, $brain_{2\ min}/brain_{60\ min}$ ratio: 8.20) and [^{99m}Tc]**4** (2.30 ± 0.27% ID/g at 2 min, $brain_{2\ min}/brain_{60\ min}$ ratio: 4.18) showed excellent initial uptakes and fast clearance in the brain, while [^{99m}Tc]**5** (1.11 ± 0.34% ID/g at 2 min, $brain_{2\ min}/brain_{60\ min}$ ratio: 1.73) was also good as an ^{99m}Tc-labeled ligand for Aβ imaging. Meanwhile, [^{99m}Tc]**3**–**5** are probably substrates for the rodent PgP transporter. Therefore, the pretreating BBB abilities of these complexes are more remarkable with the PgP blocked. These findings suggest that additional effort should be made to explore why these kinds of complexes can penetrate the BBB more efficiently than other ^{99m}Tc-labeled ligands, which may lead to some new suggestions about how to design ^{99m}Tc-labeled CNS probes. In conclusion, these small technetium-99m complexes (<500 Da) designed by an integrated approach mimicking chalcone provide encouraging

dx.doi.org/10.1021/jm3014184 | J. Med. Chem. 2013, 56, 471–482

Table 4. Biodistribution of [^{99m}Tc]3 in Male ICR Mice[a]

	time after injection				
organ	2 min	10 min	30 min	60 min	120 min
blood	2.02 ± 0.17	0.82 ± 0.05	0.51 ± 0.07	0.51 ± 0.06	0.44 ± 0.08
brain	4.10 ± 0.38	2.27 ± 0.51	0.69 ± 0.09	0.50 ± 0.08	0.37 ± 0.08
heart	11.47 ± 1.65	1.87 ± 0.36	0.98 ± 0.22	0.84 ± 0.16	0.55 ± 0.15
liver	18.14 ± 1.77	24.75 ± 3.38	22.43 ± 4.39	25.96 ± 2.06	25.24 ± 5.17
spleen	3.53 ± 0.52	1.93 ± 0.30	0.81 ± 0.14	0.64 ± 0.14	0.51 ± 0.15
lung	7.39 ± 1.06	7.32 ± 0.71	5.52 ± 0.49	5.38 ± 0.38	4.79 ± 0.43
kidney	13.36 ± 0.99	5.38 ± 0.66	3.87 ± 0.79	3.17 ± 0.16	2.56 ± 0.40
stomach[b]	1.69 ± 0.16	3.06 ± 0.90	2.18 ± 0.39	1.38 ± 0.55	0.75 ± 0.16
small intestine[b]	6.81 ± 1.57	17.98 ± 1.58	37.71 ± 7.94	34.75 ± 2.26	26.22 ± 4.20

[a]Expressed as % injected dose per gram. Average for 5 mice ± standard deviation. [b]Expressed as % injected dose per organ.

Table 5. Biodistribution of [^{99m}Tc]4 in Male ICR Mice[a]

	time after injection				
organ	2 min	10 min	30 min	60 min	120 min
blood	3.80 ± 0.71	1.25 ± 0.17	0.98 ± 0.49	0.64 ± 0.15	0.55 ± 0.07
brain	2.30 ± 0.27	1.85 ± 0.25	0.93 ± 0.09	0.55 ± 0.08	0.49 ± 0.11
heart	12.94 ± 2.16	3.58 ± 0.51	1.92 ± 0.26	1.36 ± 0.13	0.92 ± 0.12
liver	32.64 ± 4.34	28.81 ± 4.57	34.32 ± 5.35	35.93 ± 4.25	29.59 ± 5.35
spleen	4.50 ± 0.91	4.34 ± 0.92	2.84 ± 0.90	1.25 ± 0.23	1.00 ± 0.16
lung	9.08 ± 2.20	6.18 ± 1.59	4.03 ± 0.83	3.29 ± 1.45	2.74 ± 0.38
kidney	15.59 ± 1.89	6.56 ± 1.01	5.56 ± 0.94	4.31 ± 0.83	3.82 ± 0.68
stomach[b]	1.11 ± 0.24	1.28 ± 0.33	1.86 ± 0.60	1.90 ± 0.22	1.38 ± 1.63
small intestine[b]	5.27 ± 0.46	15.12 ± 5.32	24.42 ± 4.62	34.63 ± 4.72	29.94 ± 5.47

[a]Expressed as % injected dose per gram. Average for 5 mice ± standard deviation. [b]Expressed as % injected dose per organ.

Table 6. Biodistribution of [^{99m}Tc]5 in Male ICR Mice[a]

	time after injection				
organ	2 min	10 min	30 min	60 min	120 min
blood	13.53 ± 1.37	1.01 ± 0.11	0.70 ± 0.08	0.82 ± 0.06	0.98 ± 0.22
brain	1.11 ± 0.34	0.40 ± 0.05	0.38 ± 0.05	0.51 ± 0.08	0.64 ± 0.11
heart	11.48 ± 1.82	3.50 ± 0.23	2.61 ± 0.28	1.70 ± 0.14	1.73 ± 0.24
liver	52.40 ± 3.64	67.08 ± 3.54	57.20 ± 3.09	40.49 ± 6.00	42.91 ± 3.43
spleen	13.14 ± 2.57	21.59 ± 2.91	20.95 ± 2.72	18.63 ± 4.75	11.65 ± 4.25
lung	31.98 ± 4.58	13.89 ± 1.39	8.66 ± 0.99	9.69 ± 0.52	9.18 ± 1.87
kidney	7.11 ± 0.80	2.83 ± 0.33	2.87 ± 0.73	2.98 ± 0.36	4.12 ± 0.56
stomach[b]	0.63 ± 0.10	0.50 ± 0.06	0.74 ± 0.08	0.93 ± 0.12	1.15 ± 0.13
small intestine[b]	2.30 ± 0.45	3.84 ± 0.48	9.85 ± 0.72	16.64 ± 2.29	14.93 ± 2.70

[a]Expressed as % injected dose per gram. Average for 5 mice ± standard deviation. [b]Expressed as % injected dose per organ.

Table 7. Biodistribution of [^{99m}Tc]3−5 at 2 min with/without PgP Blocked by Cyclosporin A in Male ICR Mice[a]

organ	[^{99m}Tc]**3**	[^{99m}Tc]**3**[b]	[^{99m}Tc]**4**	[^{99m}Tc]**4**[b]	[^{99m}Tc]**5**	[^{99m}Tc]**5**[b]
blood	2.02 ± 0.17	4.20 ± 0.37	3.80 ± 0.71	4.24 ± 0.19	13.53 ± 1.37	13.07 ± 1.01
brain	4.10 ± 0.38	6.34 ± 0.81	2.30 ± 0.27	3.68 ± 0.07	1.11 ± 0.34	1.64 ± 0.17

[a]Expressed as % injected dose per gram. Average for 5 mice ± standard deviation. [b]Biodistribution of [^{99m}Tc]**3-5** at 2 min with PgP blocked by Cyclosporin A in male ICR mice

evidence that development of a ^{99m}Tc-labeled agent for imaging Aβ plaques in the brain may be feasible.

EXPERIMENTAL SECTION

General Information. All reagents used in the synthesis were commercial products and were used without further purification unless otherwise indicated. The ^{99m}Tc−pertechnetate was eluted from a commercial ^{99}Mo/^{99m}Tc generator which was obtained from Beijing Atomic High-Tech Co. The ^{1}H NMR spectra were obtained at 400 MHz on a Bruker spectrometer in $CDCl_3$ at room temperature with TMS as an internal standard. Chemical shifts were reported as δ values with respect to residual solvents. The ^{13}C NMR spectra were obtained at 100 MHz on Bruker spectrometer in $CDCl_3$ at room temperature. Chemical shifts were reported as δ values with respect to residual solvents. The multiplicity is defined by s (singlet), d (doublet), t (triplet), m (multiplet). Mass spectrometry was acquired under the Surveyor MSQ Plus (ESI) (Waltham, MA, USA) instrument. X-ray crystallography data were collected on a Bruker Smart APEX II diffractometer (Bruker Co., Germany). Reactions were monitored by TLC (TLC Silica gel 60 F_{254}, Merck). Radiochemical purity was determined by HPLC performed on a Shimadzu SCL-20 AVP

dx.doi.org/10.1021/jm3014184 | J. Med. Chem. 2013, 56, 471−482

equipped with a Bioscan Flow Count 3200 NaI/PMT γ-radiation scintillation detector. Separations were achieved on a Venusil MP C18 column (Agela Technologies, 10 μm, 10 mm ×250 mm) eluted with a binary gradient system at a 4.0 mL/min flow rate. Mobile phase A was water, while mobile phase B was acetonitrile. Fluorescent observation was performed by Axio Oberver Z1 (Zeiss, Germany) equipped with DAPI (excitation, 405 nm) and GFP filter sets (excitation, 505 nm). The purity of the synthesized key compounds was determined using analytical HPLC and was found to be more than 95%. Normal ICR mice (five weeks, male) were used for biodistribution experiments. All protocols requiring the use of mice were approved by the animal care committee of Beijing Normal University. Post-mortem brain tissues from an autopsy-confirmed case of AD (91-year-old, male, 35 μm, prefrontal cortex) and a control subject (69-year-old, female, 35 μm, prefrontal cortex) were kindly gifted from Dr. Jiapei Dai, which were obtained from The Netherlands Brain Bank (NBB) by autopsy. Transgenic mice brain tissues (C57BL6, APPswe/PSEN1, 11 months old, male) were purchased from Institute of Laboratory Animal Sciences, Chinese Academy of Medical Sciences.

Chemistry. *(2E,4E)-5-(4-(Dimethylamino)phenyl)penta-2,4-dienal (**1**).* To a stirring solution of (*E*)-3-(4-(dimethylamino)phenyl)-acrylaldehyde (526 mg, 3.0 mmol) in dry THF, (1,3-dioxolan-2-yl)methyltriphenylphosphonium (1.55 g, 3.6 mmol) was added to form a suspension at room temperature, followed by 18-crown-6 (79 mg, 0.3 mmol) and NaH (60% in paraffin wax, 200 mg, 5.0 mmol) in a ice bath. The reaction was then stirred under room temperature for 2 h until quenched by adding 2.0 mL of concentrated hydrochloric acid. Thirty minutes later, the solution was neutralized with saturated K_2CO_3 aqueous solution and extracted with ethyl acetate (3 × 50 mL). The organic layer was dried over Na_2SO_4. After the solvent was removed, the residue was purified by silica gel chromatography (ethyl acetate/petroleum ether = 6:1, v/v) to afford the final products (yield 55%). ^{1}H NMR ($CDCl_3$, 400 MHz): δ 3.05 (s, 6H), 6.15−6.20 (m, 1H), 6.51−6.57 (m, 1H), 6.68−6.96 (m, 3H), 7.22−7.46 (m, 3H), 9.55−9.60 (m, 1H). MS: *m*/*z* calcd for $[C_{13}H_{15}NO + H]^+$ 202.1; found 202.4.

*(Acetylcyclopentadienyl)tricarbonylrhenium (**2**).* To a stirring solution of (cyclopentadienyl)tricarbonylrhenium (200 mg, 0.6 mmol) in dry CH_2Cl_2 in ice bath, acetyl chloride (94 mg, 1.2 mmol) was added dropwise. The reaction mixture was stirred for 30 min at 0 °C and 30 min at room temperature. After adding 50 mL of water, the mixture was extracted with ethyl acetate (3 × 30 mL). The organic layer was dried over Na_2SO_4. The solvent was removed to afford the white solid products (yield 95%). ^{1}H NMR ($CDCl_3$, 400 MHz): δ 2.34 (s, 3H), 5.40 (t, *J* = 2.3 Hz, 2H), 5.98 (t, *J* = 2.3 Hz, 2H). MS: *m*/*z* calcd for $[C_{10}H_7O_4{}^{187}Re + H]^+$ 379.0; found 379.1.

*1-[(2E)-1-Oxo-3-(4-dimethylaminophenyl)-2-propenyl]-(cyclopentadienyl)tricarbonylrhenium (**3**).* Complex **2** (50 mg, 0.15 mmol), 4-(dimethylamino)benzaldehyde (30 mg, 0.2 mmol), and solid NaOH (40 mg, 1.0 mmol) were dissolved in anhydrous ethanol (5 mL). The mixture was stirred at room temperature for 6 h until stopping by adding 30 mL of water. After extraction with ethyl acetate, the solvent was removed under reduced pressure. The residue was purified by silica gel chromatography (ethyl acetate/petroleum ether = 1:1, v/v) to afford a yellow solid. The solid was crystallized from a mixture of ethanol and dichloromethane as light-yellow crystals (yield 91%); mp 180.2−182.4 °C. ^{1}H NMR ($CDCl_3$, 400 MHz): δ 3.05 (s, 6H), 5.41 (t, *J* = 2.3 Hz, 2H), 6.09 (t, *J* = 2.3 Hz, 2H), 6.68 (d, *J* = 8.9 Hz, 2H), 6.73 (d, *J* = 15.3 Hz, 2H), 7.50 (d, *J* = 8.8 Hz, 1H), 7.78 (d, *J* = 15.3 Hz, 1H). ^{13}C NMR ($CDCl_3$, 100 MHz): δ 40.1, 84.6, 87.8, 98.8, 111.8, 114.9, 122.0, 130.7, 145.6, 152.3, 183.8, 192.3. HRMS: *m*/*z* calcd for $[C_{19}H_{16}NO_4{}^{187}Re + H]^+$ 510.0715; found 510.0717.

*1-[(2E,4E)-1-Oxo-5-(4-dimethylaminophenyl)-2,4-pentadienyl]-(cyclopentadienyl)tricarbonylrhenium (**4**).* Complex **4** was prepared following the procedure used for **3**. The residue was purified by silica gel chromatography (ethyl acetate/petroleum ether = 1:1, v/v) to afford an orange solid. The solid was crystallized from a mixture of ethanol and dichloromethane as light-orange crystals (yield 87%); mp 217.6−218.4 °C. ^{1}H NMR ($CDCl_3$, 400 MHz): δ 3.02 (s, 6H), 5.40 (t, *J* = 2.3 Hz, 2H), 6.04 (t, *J* = 2.3 Hz, 2H), 6.39 (d, *J* = 14.6 Hz, 1H), 6.67 (d, *J* = 8.8 Hz, 2H), 6.77 (dd, J_1 = 15.3 Hz, J_2 = 11.3 Hz, 1H), 6.97 (d, *J* = 15.4 Hz, 1H), 7.39 (d, *J* = 8.8 Hz, 2H), 7.61 (dd, J_1 = 14.6 Hz, J_2 = 11.3 Hz, 1H). ^{13}C NMR ($CDCl_3$, 100 MHz): δ 40.2, 85.0, 87.7, 98.5, 111.9, 120.6, 121.8, 123.7, 129.1, 144.3, 146.2, 151.3, 183.8, 192.2. HRMS: *m*/*z* calcd for $[C_{21}H_{18}NO_4{}^{187}Re + H]^+$ 536.0872; found 536.0859.

*1-[(2E,4E,6E)-1-Oxo-7-(4-dimethylaminophenyl)-2,4,6-heptatrienyl)]-(cyclopentadienyl)tricarbonylrhenium (**5**).* Complex **5** was prepared following the procedure used for **3**. The residue was purified by silica gel chromatography (ethyl acetate/petroleum ether = 1:1, v/v) to afford a red solid (yield 85%); mp 205.2−207.2 °C. ^{1}H NMR ($CDCl_3$, 400 MHz): δ 3.00 (s, 6H), 5.40 (s, 2H), 6.04 (s, 2H), 6.32−6.44 (m, 2H), 6.67 (d, *J* = 8.8 Hz, 2H), 6.72−6.74 (m, 2H), 6.82−6.88 (m, 1H), 7.34−7.40 (m, 2H), 7.53 (dd, J_1 = 14.5 Hz, J_2 = 11.8 Hz, 1H). ^{13}C NMR ($CDCl_3$, 100 MHz): δ 40.2, 85.1, 87.7, 98.3, 112.1, 121.5, 123.9, 124.7, 127.9, 128.8, 138.9, 145.1, 145.5, 150.8, 183.8, 192.1. HRMS: *m*/*z* calcd for $[C_{23}H_{20}NO_4{}^{187}Re + H]^+$ 562.1028; found 562.1030.

*1-[(2E,4E)-1-Oxo-5-(4-dimethylaminophenyl)-2,4-pentadienyl]-ferrocene (**6**).* Acetylferrocene (35 mg, 0.15 mmol), (*E*)-3-(4-(dimethylamino)phenyl)acrylaldehyde (35 mg, 0.20 mmol), and solid NaOH (40 mg, 1.0 mmol) were dissolved in anhydrous ethanol (5 mL). The mixture was stirred at room temperature for 6 h. After filtration, the solvent was removed under reduced pressure. The residue was purified by silica gel chromatography (ethyl acetate/petroleum ether = 1:1, v/v) to afford a dark-red solid (yield 90%). ^{1}H NMR ($CDCl_3$, 400 MHz): δ 3.01 (s, 6H), 4.20 (s, 5H), 4.53 (s, 2H), 4.86 (s, 2H), 6.53−6.98 (m, 5H), 7.32−7.79 (m, 3H). MS: *m*/*z* calcd for $[C_{23}H_{23}FeNO_4 + H]^+$ 386.1; found 386.5.

*1-[(2E,4E,6E)-1-Oxo-7-(4-dimethylaminophenyl)-2,4,6-heptatrienyl)]-ferrocene (**7**).* Complex **7** was prepared following the procedure used for **6**. The residue was purified by silica gel chromatography (ethyl acetate/petroleum ether = 1:1, v/v) to afford a brown solid (yield 88%). ^{1}H NMR ($CDCl_3$, 400 MHz): δ 3.01 (s, 6H), 4.20 (s, 5H), 4.54 (s, 2H), 4.85 (s, 2H), 6.53−6.50 (m, 1H), 6.56 (d, *J* = 14.8 Hz, 1H), 6.64−6.86 (m, 4H), 6.79−6.86(m, 1H), 7.33−7.37 (m, 2H), 7.47−7.54(m, 1H). MS: *m*/*z* calcd for $[C_{25}H_{25}FeNO_4 + H]^+$ 412.1; found 412.6.

X-ray Crystallography. Single-crystal X-ray diffraction measurements were carried out on a Bruker Smart APEXII CCD diffractometer at 150(2) K using graphite monochromated Mo Kα radiation (λ = 0.71070 Å). An empirical absorption correction was applied using the SADABS program.[39] All structures were solved by direct methods and refined by full-matrix least-squares on F^2 using the SHELXL-97 program package.[40] All of the hydrogen atoms were geometrically fixed using the riding model.

In Vitro Fluorescent Staining of Aβ Plaques in Transgenic Mouse Brain Sections and Human Brain Materials. Paraffin-embedded brain sections of Tg mouse (C57BL6, APPswe/PSEN1, 11 months old, male, 6 μm) were used for the fluorescent staining. The brain sections were deparaffinized with 2 × 20 min washes in xylene, 2 × 5 min washes in 100% ethanol, 5 min washes in 90% ethanol/H_2O, 5 min wash in 80% ethanol/H_2O, 5 min wash in 60% ethanol/H_2O, and running tap water for 10 min and then incubated in PBS (0.2 M, pH = 7.4) for 30 min. The sections of human prefrontal cortex (35 μm) were obtained from The Netherlands Brain Bank (NBB) by autopsy, and the sections were stored at 0−4 °C in 50% glycerol diluted with 0.05 M TBS before use.

The brain sections were incubated with 10% ethanol solution (1.0 μM) of **3**, **4**, and **5** for 10 min. The localization of plaques was confirmed by staining with thioflavin-S (0.125%) on the adjacent sections. Finally, the sections were washed with 50% ethanol and PBS (0.2 M, pH = 7.4) for 10 min. Fluorescent observation was performed by Axio Oberver Z1 (Zeiss, Germany) equipped with DAPI (excitation, 405 nm) and GFP filter sets (excitation, 505 nm).

Binding Assay in Vitro Using Aβ Aggregates. The trifluoroacetic acid salt forms of peptides Aβ_{1-42} were purchased from AnaSpec. Aggregation of peptides was carried out by gently dissolving the peptide (0.25 mg/mL for Aβ_{1-42}) in a buffer solution (pH = 7.4) containing 10 mM potassium dihydrogen phosphate and 1 mM

dx.doi.org/10.1021/jm3014184 | J. Med. Chem. 2013, 56, 471−482

EDTA. The solutions were incubated at 37 °C for 42 h with gentle and constant shaking. Inhibition experiments were carried out in 12 mm × 75 mm borosilicate glass tubes according to procedures described previously with some modification.[17] Briefly, 100 μL of aggregated Aβ fibrils (28 nM in the final assay mixture) was added to a mixture containing 100 μL of radioligand ([^{125}I]IMPY, 100000 cpm/100 μL), 100 μL of inhibitors (complexes **3**, **4**, or **5**, 10^{-4} M to 10^{-10} M in ethanol), and 700 μL of PBS (0.2 M, pH = 7.4) in a final volume of 1.0 mL. Nonspecific binding was defined in the presence of 1 μM IMPY. The mixture was incubated for 2 h at 37 °C, and then the bound and free radioactive fractions were separated by vacuum filtration through borosilicate glass fiber filters (Whatman GF/B) using a Mp-48T cell harvester (Brandel, Gaithersburg, MD). The radioactivity from filters containing the bound ^{125}I-ligand was measured in a γ-counter (WALLAC/Wizard1470, USA) with 70% efficiency. Under the assay conditions, the specifically bound fraction accounted for about 10% of total radioactivity. The inhibitory concentration (IC_{50}) was determined using Graph Pad Prism 4.0, and the inhibition constant (K_i) was calculated using the Cheng–Prusoff inhibition constant equation: $K_i = IC_{50}/(1 + [L]/K_d)$.[41]

Preparation of [^{99m}Tc]3, [^{99m}Tc]4, and [^{99m}Tc]5. To an orange solution of 1.0 mg of acetylferrocene and 1.0 mg of $Mn(CO)_5Br$ in 1 mL of DMF, 1.0 mL of $^{99m}TcO_4^-$ aqueous solution (10 mCi) were added. The reaction mixture was kept at 150 °C for 20 min in a sealed vial. After extraction with CH_2Cl_2 and water, inorganic salts were separated from the product while the intermediate [^{99m}Tc]**2** was saved in CH_2Cl_2. After removing the CH_2Cl_2 under nitrogen gas, the residue was dissolved again in 1.0 mL of absolute ethanol. The appropriate aldehyde (3.0 mg) was added into the reaction as well as 0.5 mg NaOH to catalyze the Claisen Condensation. The reaction was kept under room temperature for 30 min. After extraction by CH_2Cl_2, the solvent was evaporated under nitrogen gas and the residue was dissolved in CH_3CN and purified by radio-HPLC under conditions as following: Venusil MP C18 column (Agela Technologies, 10 mm × 250 mm), CH_3CN/H_2O = 70/30 for [^{99m}Tc]**3**, [^{99m}Tc]**4**, CH_3CN/H_2O = 80/20 for [^{99m}Tc]**5**, 4 mL/min, UV = 254 nm.

Binding Assay Using Aβ Aggregates with [^{99m}Tc]2–5. The binding assay was performed by mixing 100 μL of [^{99m}Tc]**2**–**5** (100000 cpm/100 μL), 100 μL of $A\beta_{1-42}$ aggregates (7.27 μg/mL), and 800 μL of 10% ethanol in 12 mm × 75 mm borosilicate glass tubes. The blocking assay was performed by conducting the binding assay in the presence of excess of rhenium complexes **2**–**5** (1 μM for **2**–**4**, 0.5 μM for **5**) as blocking agents. After incubation for 2 h at room temperature, the mixture was filtered through GF/B filters (Whatman GF/B) using a Mp-48T cell harvester (Brandel, Gaithersburg, MD). Filters containing the bound ^{99m}Tc-labeled form were examined in an automatic γ-counter (Wallac 1470 Wizard, USA).

Autoradiography in Vitro Using Brain Sections of Human and Transgenic Model Mouse. Paraffin-embedded brain sections of Tg and control mice were deparaffinized with 2 × 20 min washes in xylene, 2 × 5 min washes in 100% ethanol, a 5 min wash in 90% ethanol/H_2O, a 5 min wash in 80% ethanol/H_2O, a 5 min wash in 60% ethanol/H_2O, and a 10 min wash in running tap water and then incubated in PBS (0.2 M, pH = 7.4) for 30 min. The sections were incubated with [^{99m}Tc]**5** (370 KBq/100 μL) for 1 h at room temperature. They were then washed in 40% EtOH before being rinsed with water for 1 min. After drying, the sections were exposed to a phosphorus plate (Perkin-Elmer, USA) for 4 h. In vivo autoradiographic images were obtained using a phosphor imaging system (Cyclone, Packard). After autoradiographic examination, the same mouse brain sections were stained by thioflavin-S to confirm the presence of Aβ plaques. After drying, the fluorescent observation was performed by Axio Oberver Z1 (Zeiss, Germany) equipped with DAPI (excitation, 405 nm) and GFP filter sets (excitation, 505 nm).

Biodistribution Studies. A saline solution containing the HPLC-purified ^{99m}Tc-labeled tracer (100 μL, 10% ethanol, 5 μCi) was injected via tail vein of ICR mice (five weeks, male). The mice were sacrificed exactly at 2, 10, 30, 60, and 120 min. Samples of blood and organs of interest were removed, weighed, and counted in an automatic γ-counter (Wallac 1470 Wizard, USA). The results were expressed in terms of the percentage of the injected dose per gram (% ID/g) of blood or organs.

The biodistribution with PgP blocked was conducted using male ICR mice (5 weeks, male, n = 5) pretreated with Cyclosporin A (manufactured by Nanjing Duly biotech Co., Ltd. USP grade). Each mouse was injected via tail vein with 50 mg/kg (100 μL solution consisting of 10% EtOH, 15% saline and 75% propylene glycol), 1 h prior to administration of [^{99m}Tc]**3**–**5**.[42] The blood and brain uptakes at 2 min were measured the same way narrated before.

Partition Coefficient Determination. The determination of partition coefficients of ^{99m}Tc-labeled complexes were performed according to the procedure previously reported.[19] A solution of ^{99m}Tc-labeled complexes (1.5 MBq) was added to a premixed suspensions containing 3.0 g n-octanol and 3.0 g PBS (0.05 M, pH = 7.4) in a test tube. The test tube was vortexed for 3 min at room temperature, followed by centrifugation for 5 min at 3000 rpm. Two samples from the n-octanol (50 μL) and water (500 μL) layers were measured. The partition coefficient was expressed as the logarithm of the ratio of the count per gram from n-octanol versus PBS. Samples from the n-octanol layer were repartitioned until consistent partition coefficient values were obtained. The measurement was done in triplicate and repeated three times.

■ ASSOCIATED CONTENT

Ⓢ Supporting Information

Purities of key target compounds; HPLC profiles of **3**, [^{99m}Tc]**3**, **4**, [^{99m}Tc]**4**, **5**, [^{99m}Tc]**5**; ^{1}H NMR spectra, ^{13}C NMR spectra and HRMS data of rhenium complexes; crystal parameters for complex **3** and **4**. This material is available free of charge via the Internet at http://pubs.acs.org.

■ AUTHOR INFORMATION

Corresponding Author

*Phone: +86-10-58808891. Fax: +86-10-58808891. E-mail: cmc@bnu.edu.cn (M.C.); liuboli@bnu.edu.cn (B.L.).

Notes

The authors declare no competing financial interest.

■ ACKNOWLEDGMENTS

We present special thanks to Dr. Jin Liu (College of Life Science, Beijing Normal University) for assistance in the in vitro neuropathological staining and Dr. Xuebing Deng (College of Chemistry, Beijing Normal University) for assistance in the X-ray diffraction. This work was supported by National Natural Science Foundation of China (grants 21201019, 20871021, and 31070961) and Research Fund for the Doctoral Program of Higher Education of China (20120003120013).

■ ABBREVIATIONS USED

Aβ, β-amyloid; AD, Alzheimer's Disease; PET, positron emission tomography; SPECT, single photon emission computed tomography; CNS, central nervous system; BBB, blood–brain barrier; DLT, double ligand transfer; Cp, cyclopentadienyl; MAMA, monoamine-monoamide dithiol; BAT, bis-amino-bis-thiol; HPLC, high performance liquid chromatography; NBB, Netherlands Brain Bank; PgP, permeability-glycoprotein 1

■ REFERENCES

(1) Selkoe, D. J. Imaging Alzheimer's amyloid. *Nature Biotechnol.* **2000**, *18*, 823–824.

(2) Mathis, C. A.; Wang, Y.; Klunk, W. E. Imaging beta-amyloid plaques and neurofibrillary tangles in the aging human brain. *Curr. Pharm. Des.* **2004**, *10*, 1469–1492.

(3) Nordberg, A. PET imaging of amyloid in Alzheimer's disease. *Lancet Neurol.* **2004**, *3*, 519−527.
(4) Agdeppa, E. D.; Kepe, V.; Liu, J.; Flores-Torres, S.; Satyamurthy, N.; Petric, A.; Cole, G. M.; Small, G. W.; Huang, S. C.; Barrio, J. R. Binding characteristics of radiofluorinated 6-dialkylamino-2-naphthylethylidene derivatives as positron emission tomography imaging probes for beta-amyloid plaques in Alzheimer's disease. *J. Neurosci.* **2001**, *21*, RC189.
(5) Shoghi-Jadid, K.; Small, G. W.; Agdeppa, E. D.; Kepe, V.; Ercoli, L. M.; Siddarth, P.; Read, S.; Satyamurthy, N.; Petric, A.; Huang, S. C.; Barrio, J. R. Localization of neurofibrillary tangles and beta-amyloid plaques in the brains of living patients with Alzheimer disease. *Am. J. Geriatr. Psychiatry* **2002**, *10*, 24−35.
(6) Mathis, C. A.; Wang, Y.; Holt, D. P.; Huang, G. F.; Debnath, M. L.; Klunk, W. E. Synthesis and evaluation of 11C-labeled 6-substituted 2-arylbenzothiazoles as amyloid imaging agents. *J. Med. Chem.* **2003**, *46*, 2740−2754.
(7) Klunk, W. E.; Engler, H.; Nordberg, A.; Wang, Y.; Blomqvist, G.; Holt, D. P.; Bergstrom, M.; Savitcheva, I.; Huang, G. F.; Estrada, S.; Ausen, B.; Debnath, M. L.; Barletta, J.; Price, J. C.; Sandell, J.; Lopresti, B. J.; Wall, A.; Koivisto, P.; Antoni, G.; Mathis, C. A.; Langstrom, B. Imaging brain amyloid in Alzheimer's disease with Pittsburgh Compound-B. *Ann. Neurol.* **2004**, *55*, 306−319.
(8) Ono, M.; Wilson, A.; Nobrega, J.; Westaway, D.; Verhoeff, P.; Zhuang, Z. P.; Kung, M. P.; Kung, H. F. 11C-labeled stilbene derivatives as Abeta-aggregate-specific PET imaging agents for Alzheimer's disease. *Nucl. Med. Biol.* **2003**, *30*, 565−571.
(9) Verhoeff, N. P.; Wilson, A. A.; Takeshita, S.; Trop, L.; Hussey, D.; Singh, K.; Kung, H. F.; Kung, M. P.; Houle, S. In vivo imaging of Alzheimer disease beta-amyloid with [11C]SB-13 PET. *Am. J. Geriatr. Psychiatry* **2004**, *12*, 584−595.
(10) Okamura, N.; Shiga, Y.; Furumoto, S.; Tashiro, M.; Tsuboi, Y.; Furukawa, K.; Yanai, K.; Iwata, R.; Arai, H.; Kudo, Y.; Itoyama, Y.; Doh-ura, K. In vivo detection of prion amyloid plaques using [(11)C]BF-227 PET. *Eur. J. Nucl. Med. Mol. Imaging* **2010**, *37*, 934−941.
(11) Rowe, C. C.; Ackerman, U.; Browne, W.; Mulligan, R.; Pike, K. L.; O'Keefe, G.; Tochon-Danguy, H.; Chan, G.; Berlangieri, S. U.; Jones, G.; Dickinson-Rowe, K. L.; Kung, H. P.; Zhang, W.; Kung, M. P.; Skovronsky, D.; Dyrks, T.; Holl, G.; Krause, S.; Friebe, M.; Lehman, L.; Lindemann, S.; Dinkelborg, L. M.; Masters, C. L.; Villemagne, V. L. Imaging of amyloid beta in Alzheimer's disease with 18F-BAY94−9172, a novel PET tracer: proof of mechanism. *Lancet Neurol.* **2008**, *7*, 129−135.
(12) Choi, S. R.; Golding, G.; Zhuang, Z.; Zhang, W.; Lim, N.; Hefti, F.; Benedum, T. E.; Kilbourn, M. R.; Skovronsky, D.; Kung, H. F. Preclinical properties of 18F-AV-45: a PET agent for Abeta plaques in the brain. *J. Nucl. Med.* **2009**, *50*, 1887−1894.
(13) Kung, H. F.; Choi, S. R.; Qu, W.; Zhang, W.; Skovronsky, D. 18F stilbenes and styrylpyridines for PET imaging of A beta plaques in Alzheimer's disease: a miniperspective. *J. Med. Chem.* **2010**, *53*, 933−941.
(14) Kung, M. P.; Hou, C.; Zhuang, Z. P.; Zhang, B.; Skovronsky, D.; Trojanowski, J. Q.; Lee, V. M.; Kung, H. F. IMPY: an improved thioflavin-T derivative for in vivo labeling of beta-amyloid plaques. *Brain Res.* **2002**, *956*, 202−210.
(15) Zhuang, Z. P.; Kung, M. P.; Wilson, A.; Lee, C. W.; Plossl, K.; Hou, C.; Holtzman, D. M.; Kung, H. F. Structure−activity relationship of imidazo[1,2-*a*]pyridines as ligands for detecting beta-amyloid plaques in the brain. *J. Med. Chem.* **2003**, *46*, 237−243.
(16) Newberg, A. B.; Wintering, N. A.; Plossl, K.; Hochold, J.; Stabin, M. G.; Watson, M.; Skovronsky, D.; Clark, C. M.; Kung, M. P.; Kung, H. F. Safety, biodistribution, and dosimetry of 123I-IMPY: a novel amyloid plaque-imaging agent for the diagnosis of Alzheimer's disease. *J. Nucl. Med.* **2006**, *47*, 748−754.
(17) Qu, W.; Kung, M. P.; Hou, C.; Benedum, T. E.; Kung, H. F. Novel styrylpyridines as probes for SPECT imaging of amyloid plaques. *J. Med. Chem.* **2007**, *50*, 2157−2165.
(18) Watanabe, H.; Ono, M.; Haratake, M.; Kobashi, N.; Saji, H.; Nakayama, M. Synthesis and characterization of novel phenylindoles as potential probes for imaging of beta-amyloid plaques in the brain. *Bioorg. Med. Chem.* **2010**, *18*, 4740−4746.
(19) Cui, M.; Ono, M.; Kimura, H.; Kawashima, H.; Liu, B. L.; Saji, H. Radioiodinated benzimidazole derivatives as single photon emission computed tomography probes for imaging of beta-amyloid plaques in Alzheimer's disease. *Nucl. Med. Biol.* **2011**, *38*, 313−320.
(20) Kung, H. F.; Kim, H. J.; Kung, M. P.; Meegalla, S. K.; Plossl, K.; Lee, H. K. Imaging of dopamine transporters in humans with technetium-99m TRODAT-1. *Eur. J. Nucl. Med.* **1996**, *23*, 1527−1530.
(21) Han, H.; Cho, C. G.; Lansbury, P. T. Technetium complexes for the quantitation of brain amyloid. *J. Am. Chem. Soc.* **1996**, *118*, 4506−4507.
(22) Zhuang, Z. P.; Kung, M. P.; Hou, C.; Ploessl, K.; Kung, H. F. Biphenyls labeled with technetium 99m for imaging beta-amyloid plaques in the brain. *Nucl. Med. Biol.* **2005**, *32*, 171−184.
(23) Liu, S.; Edwards, D. S. 99mTc-Labeled small peptides as diagnostic radiopharmaceuticals. *Chem. Rev.* **1999**, *99*, 2235−2268.
(24) Dezutter, N. A.; Dom, R. J.; de Groot, T. J.; Bormans, G. M.; Verbruggen, A. M. 99mTc-MAMA-chrysamine G, a probe for beta-amyloid protein of Alzheimer's disease. *Eur. J. Nucl. Med.* **1999**, *26*, 1392−1399.
(25) Dezutter, N. A.; Sciot, R. M.; de Groot, T. J.; Bormans, G. M.; Verbruggen, A. M. In vitro affinity of 99Tcm-labelled N2S2 conjugates of chrysamine G for amyloid deposits of systemic amyloidosis. *Nucl. Med. Commun.* **2001**, *22*, 553−558.
(26) Serdons, K.; Verduyckt, T.; Cleynhens, J.; Terwinghe, C.; Mortelmans, L.; Bormans, G.; Verbruggen, A. Synthesis and evaluation of a 99mTc-BAT-phenylbenzothiazole conjugate as a potential in vivo tracer for visualization of amyloid beta. *Bioorg. Med. Chem. Lett.* **2007**, *17*, 6086−6090.
(27) Chen, X. J.; Yu, P. R.; Zhang, L. F.; Liu, B. Synthesis and biological evaluation of Tc-99m, Re-monoamine-monoamide conjugated to 2-(4-aminophenyl) benzothiazole as potential probes for beta-amyloid plaques in the brain. *Bioorg. Med. Chem. Lett.* **2008**, *18*, 1442−1445.
(28) Lin, K. S.; Debnath, M. L.; Mathis, C. A.; Klunk, W. E. Synthesis and beta-amyloid binding properties of rhenium 2-phenylbenzothiazoles. *Bioorg. Med. Chem. Lett.* **2009**, *19*, 2258−2262.
(29) Ono, M.; Ikeoka, R.; Watanabe, H.; Kimura, H.; Fuchigami, T.; Haratake, M.; Saji, H.; Nakayama, M. Synthesis and Evaluation of Novel Chalcone Derivatives with (99m)Tc/Re Complexes as Potential Probes for Detection of beta-Amyloid Plaques. *ACS Chem. Neurosci.* **2010**, *1*, 598−607.
(30) Ono, M.; Ikeoka, R.; Watanabe, H.; Kimura, H.; Fuchigami, T.; Haratake, M.; Saji, H.; Nakayama, M. Tc-99m/Re complexes based on flavone and aurone as SPECT probes for imaging cerebral beta-amyloid plaques. *Bioorg. Med. Chem. Lett.* **2010**, *20*, 5743−5748.
(31) Wang, X.; Cui, M.; Yu, P.; Li, Z.; Yang, Y.; Jia, H.; Liu, B. Synthesis and biological evaluation of novel technetium-99m labeled phenylbenzoxazole derivatives as potential imaging probes for beta-amyloid plaques in brain. *Bioorg. Med. Chem. Lett.* **2012**, *22*, 4327−4331.
(32) Cui, M.; Tang, R.; Li, Z.; Ren, H.; Liu, B. 99mTc- and Re-labeled 6-dialkylamino-2-naphthylethylidene derivatives as imaging probes for beta-amyloid plaques. *Bioorg. Med. Chem. Lett.* **2011**, *21*, 1064−1068.
(33) Wenzel, M. Tc-99m labelling of Cymantrene analogues with different substituents. a new approach to Tc-99m radiodiagnostics. *J. Labelled Compd. Radiopharm.* **1992**, *31*, 641−650.
(34) Bernard, J.; Ortner, K.; Spingler, B.; Pietzsch, H. J.; Alberto, R. Aqueous synthesis of derivatized cyclopentadienyl complexes of technetium and rhenium directed toward radiopharmaceutical application. *Inorg. Chem.* **2003**, *42*, 1014−1022.
(35) N'Dongo, H. W.; Raposinho, P. D.; Fernandes, C.; Santos, I.; Can, D.; Schmutz, P.; Spingler, B.; Alberto, R. Preparation and biological evaluation of cyclopentadienyl-based 99mTc-complexes

[(Cp-R)99mTc(CO)$_3$] mimicking benzamides for malignant melanoma targeting. *Nucl. Med. Biol.* **2010**, *37*, 255−264.
(36) Ono, M.; Hori, M.; Haratake, M.; Tomiyama, T.; Mori, H.; Nakayama, M. Structure−activity relationship of chalcones and related derivatives as ligands for detecting of beta-amyloid plaques in the brain. *Bioorg. Med. Chem.* **2007**, *15*, 6388−6396.
(37) Ono, M.; Haratake, M.; Mori, H.; Nakayama, M. Novel chalcones as probes for in vivo imaging of beta-amyloid plaques in Alzheimer's brains. *Bioorg. Med. Chem.* **2007**, *15*, 6802−6809.
(38) Ono, M.; Watanabe, R.; Kawashima, H.; Cheng, Y.; Kimura, H.; Watanabe, H.; Haratake, M.; Saji, H.; Nakayama, M. Fluoro-pegylated chalcones as positron emission tomography probes for in vivo imaging of beta-amyloid plaques in Alzheimer's disease. *J. Med. Chem.* **2009**, *52*, 6394−6401.
(39) Sheldrick, G. M. *SADABS, Program for Empirical Absorption Correction of Area Detector Data*; University of Gottingen: Gottingen, Germany, 1996.
(40) Sheldrick, G. M. *SHELXL-97 Program for the Refinement of Crystal Structure from Diffraction Data*; University of Gottingen: Gottingen, Germany, 1997.
(41) Cheng, Y.; Prusoff, W. Relationship between the inhibition constant (K_i) and the concentration of inhibitor which causes 50% inhibition (I_{50}) of an enzymatic reaction. *Biochem. Pharmacol.* **1973**, *22*, 3099−3108.
(42) Shao, X.; Carpenter, G. M.; Desmond, T. J.; Sherman, P.; Quesada, C. A.; Fawaz, M.; Brooks, A. F.; Kilbourn, M. R.; Albin, R. L.; Frey, K. A.; Scott, P. J. H. Evaluation of [11C]*N*-Methyl Lansoprazole as a Radiopharmaceutical for PET Imaging of Tau Neurofibrillary Tangles. *ACS Med. Chem. Lett.* **2012**, *3*, 936−941.